Secondary Crystallization and Premelting Endo- and Exotherms in Oriented Polymers

S. T. Correale,[1] N. S. Murthy[2]

[1]*Honeywell International Inc., Performance Products, Colonial Heights, Virginia 23834*
[2]*Physics Department, University of Vermont, Burlington, Vermont 05405*

Received 6 May 2005; accepted 19 September 2005
DOI 10.1002/app.23267
Published online in Wiley InterScience (www.interscience.wiley.com).

ABSTRACT: Crystallization in polyamide 6 (nylon 6) fibers during annealing was studied in detail by following the changes that occurred in the neighborhood of crystalline relaxation temperatures, by using wide- and small-angle X-ray scattering and differential scanning calorimetry (DSC). Two distinct crystallization regimes were observed depending on whether annealing was carried out below or above onset of crystalline relaxation at ~190°C. In fibers annealed below 190°C, minor melting peaks were followed by exothermic transitions. These were attributed to ~1.5% (by weight) of microcrystals formed during annealing that melt and recrystallize during the DSC scan. These microcrystals are nucleated from unoriented amorphous chains between the lamellar stack within a fibril, and are shown to account for the observed increase in the crystalline orientation and decrease in permeability. Fibers annealed above 190°C did not show the exotherm and had significantly fewer microcrystals. The crystallization in this regime was attributed to the growth of existing lamellae, as evidenced by the increase in crystallite size, crystalline density, crystalline orientation, lamellar spacing, and lamellar intensity. The changes at annealing temperatures >190°C are accompanied by increased dyeability, indicative of more open amorphous regions. J Appl Polym Sci 101: 447–454, 2006

Key words: secondary crystallization; oriented polymers; nylon 6; premelting thermal transitions

INTRODUCTION

Although general features of crystallization behavior and the accompanying structural changes in semicrystalline polymers are well understood, the detailed kinetics of crystallization under various constraints is not. There is a renewed interest in the crystallization behavior on polymers, especially the secondary crystallization.[1] Thermal transitions that occur prior to melting as a result of secondary crystallizations are greatly influenced by the thermal and mechanical history. Such transitions are commonly reported as multiple endotherms observed in differential scanning calorimetry (DSC) scans of polymers as they are heated from room temperature to their melt. These multiple endotherms are reliable records of the thermomechanical history of polymers and as such are of considerable commercial significance, and have therefore been studied extensively.[2] Of particular interest among these is the occurrence of a small endothermic peak prior to the main melting peak in fibers annealed under dry conditions. This endothermic peak is generally referred to as middle endothermic peak (MEP) and the temperature at which it occurs is termed the MEPT.

The MEP has been attributed to the melting of poorly ordered polymer chains, i.e., paracrystalline or microcrystalline structures.[2] MEPT in dry annealed samples increases linearly with annealing temperature.[3] This increase is attributed to changes that occur during annealing: melting of poorly crystalline regions, followed by recrystallization upon cooling, resulting in a small increase in their overall crystalline order or perfection. The MEP usually occurs at a slightly higher temperature than the annealing temperature of the fiber.

Exothermic transition prior to the melting endotherm, similar to the MEP's, has been reported for other polymers such as PET[4] and PEEK.[5–7] Exothermic transition that occurs just before the main melting endotherm, between 190 and 195°C has also been reported in nylon 6.[8] But, there have been no reports of such premelting exothermic transition in fibers using a standard DSC. The scans from samples annealed above 190°C show the development of a large broad low temperature tail near the main melting endotherm. It has been suggested that this broad low temperature tail of the melting peak in polymers is due to melting and recrystallization, and that the exothermic transition(s) are buried under the main melting endo-

Correspondence to: N. S. Murthy (sanjeeva.murthy@uvm.edu).

Contract grant sponsor: NSF EPSCOR; contract grant number: EPS-0236976.

therm.[9] We used oscillating DSC to separate the reversible and irreversible transitions and thus examine the hidden exothermic transition(s). In this article, we investigate the changes in structure and morphology that occur during annealing of nylon 6 fibers in a dry atmosphere using wide-angle X-ray diffraction (XRD) and small angle X-ray scattering (SAXS). These changes will be correlated with the changes in temperature, size, and shape of the MEP with annealing temperature.

EXPERIMENTAL

Materials

A continuous spun nylon 6 yarn with a polymer IV of 1.35 and a M_w of about 22,000 was used for our X-ray and DSC analysis. This yarn was drawn 1.5X after conditioning (lagging) and steam-textured. The final denier of the yarn was about 1360. Denier is a measure of the cross-sectional area of the fiber; it is the mass of the fiber in gram per 9000 m of yarn; cross-sectional area of a yarn of one denier is $(9000\ \rho)^{-1}$ mm^2; where ρ is the density in g/cm^3. Suessen (dry) heat-setting process used in the manufacturing of carpet yarn was simulated by unconstrained annealing of the yarns at various temperatures in a hot air oven with the blower set at medium speed. Once the oven was stable at the set temperature, the yarns were placed in the oven for 70 s, of which 20 s was needed for the oven to restabilize at the annealing temperature.

Methods

Differential scanning calorimetry

Standard DSC scans were obtained in duplicate from 10 mg specimens. The data were collected using a Perkin–Elmer DSC-7 heated from 35 to 285°C at 20°C/min under a nitrogen purge. Seiko's RDSC-220 was used to obtain oscillating DSC data using 10 mg specimens, from −25 to 265°C at 5°C/min with a frequency of 0.015 Hz and amplitude of 5°C.

Wide-angle XRD

The fibers were chopped into <1 mm length pieces using scissors, then front loaded and packed into a standard parafocus sample holder. Since most of the fibers in this packed arrangement were parallel to the diffraction surface, the resulting XRD pattern is equivalent to an equatorial scan obtainable in transmission geometry. The strain introduced by cutting is negligible, and if any it would be expected to be the same for all the samples. The primary advantage of this method is the substantial increase in intensity in the parafocus geometry versus the transmission geometries widely used for fibers. The XRD data with Cu Kα radiation were obtained in parafocus geometry using a Philips APD 1700 diffraction system on a vertical goniometer with θ-compensating slits and a graphite monochromator in the diffracted beam. The data were collected from 15° to 28° 2θ, in steps of 0.1° with 15 s per step.

In general, the XRD scans could be profile-fitted using four crystalline peaks and one amorphous halo.[10–12] In two-step heat-set yarns, the γ crystalline fraction is seldom seen, and therefore, the data were fitted to two α crystalline peaks, labeled α_1 and α_2 corresponding to 200 and (002 + 202) reflections, and an amorphous halo. We routinely use the angular separation (in °2θ) between α_1 and α_2 peaks as an index of crystalline perfection (ICP). An increase in ICP corresponds to a decrease in the unit cell dimensions, particularly the spacing between the sheets of hydrogen bonded chains.[11,13] Scherrer equation was used to estimate a composite measure of crystallite size and perfection (CSP)

$$CSP = k\lambda/\beta \cos \theta$$

where $k = 0.9$ and β = FWHM (full-width at half-maximum) of the diffracted peak (uncorrected for instrument broadening).

The diffraction data for orientation measurements were obtained on a Philips APD 1700 vertical diffractometer operated in the transmission mode with graphite monochromatized Cu Kα, 1/4° incident and 1° receiving slits. Azimuthal scans were collected for the 0140 reflection ($2\theta \sim 77°$) and the degree of crystalline orientation was determined using the FWHM of the peaks in the azimuthal direction and the Herman's orientation function

$$f_c = (3<\cos^2\phi> - 1)/2$$

wherein, $<\cos^2\phi>$ was evaluated from the FWHM assuming that the azimuthal intensity has a Gaussian distribution.[11]

Small-angle X-ray scattering

SAXS data along the fiber axis (meridional direction) were collected on a Rigaku small-angle diffractometer with Ni filtered Cu Kα radiation and a Braun 1-D position sensitive detector. The beam was collimated using 0.2 mm pinholes and sample-to-detector distance was 325 mm, of which 200 mm was evacuated. Parasitic background was subtracted from the data, absorption effects were corrected by measuring the attenuation of the 50 Å diffraction peak of lead stearate with and without the sample (private communication, B. Crist), and no Lorentz correction was applied. The scans were analyzed by profile-fitting the data to a Gaussian peak using the program PeakFit (Jandel Scientific). The long-spacing was determined by aver-

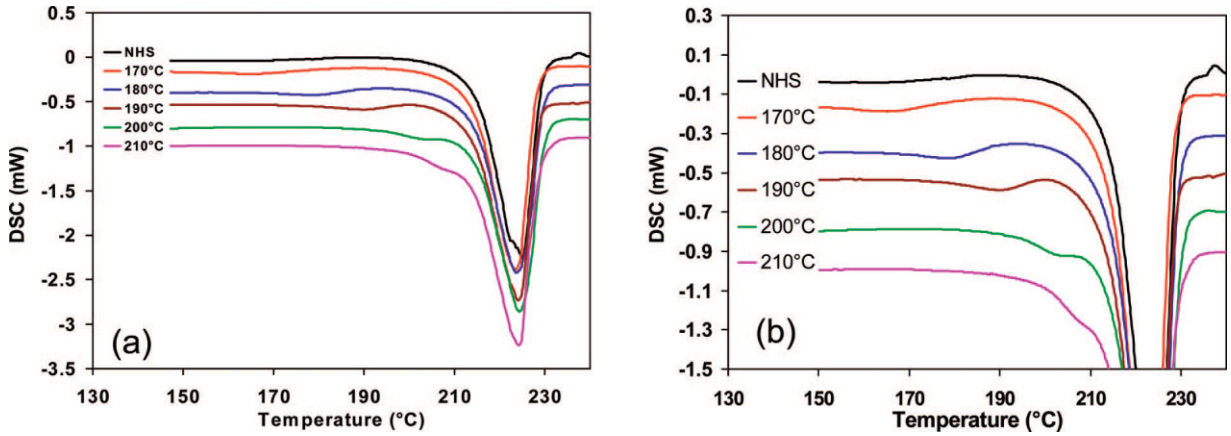

Figure 1 DSC scans from nylon 6 fibers, a nonheat set (NHS, control) fiber, and from fibers heat-set (annealed) at different temperatures as indicated in the figure. (b) The MEP region of the scans. [Color figure can be viewed in the online issue, which is available at www.interscience.wiley.com.]

aging the position of the peak maximum on both sides of the beam stop and using Bragg's law.

RESULTS

Thermal analysis

Differential scanning calorimetry

Figure 1 shows a series of normalized DSC scans of nylon 6 yarns annealed at different temperatures from 170 to 210°C. The unannealed or nonheat-set yarn is designated NHS. As the annealing temperature increases, the temperature at which the minor melting peak occurs, the MEPT, increases and size of the peak decreases. While the baseline in the NHS scan remains relatively flat almost until the main melting peak, the scan from the fiber annealed at the highest temperature shows large negative deviations from this baseline. This feature in the DSC scan, usually called a low-temperature tail of the main melting endotherm, changes significantly with annealing temperature. This tail is present in yarns annealed at high temperatures and not in those annealed at low temperatures. Difference-DSC traces were obtained by subtracting the scan of a sample annealed at a higher temperature, 210°C from a sample annealed below 190°C, for example 175°C. These traces clearly showed the presence of a broad exothermic transition (Fig. 2).

Middle endothermic peak

Figure 3 shows that the MEPT increases linearly with annealing temperature. In contrast, that heat (H_f') associated with MEP, also given in Figure 3, shows a quite different behavior. H_f' increases from that seen in NHS fibers, remains unchanged with annealing temperatures up to about 185°C, rapidly decreases between 185 and 200°C, and becomes almost constant at a very low value or decreases slightly at annealing temperatures ≥200°C. Figure 4 shows that the onset and peak temperatures of the main melting endotherm did not change significantly with annealing temperature. But, the shape and the area of the main endotherm (H_f) were affected by the presence of the hidden exothermic transition. For instance, H_f was considerably lower in samples annealed below 200°C (Fig. 4).

Oscillating DSC

Figure 5 shows the irreversible component of the heat flow from an oscillating (or modulated) DSC scans for yarn samples annealed at 180 and 210°C. There is at least one broad exothermic feature with a maximum at about 190°C in yarns annealed at 180°C. This feature is not present in yarns annealed at 210°C.

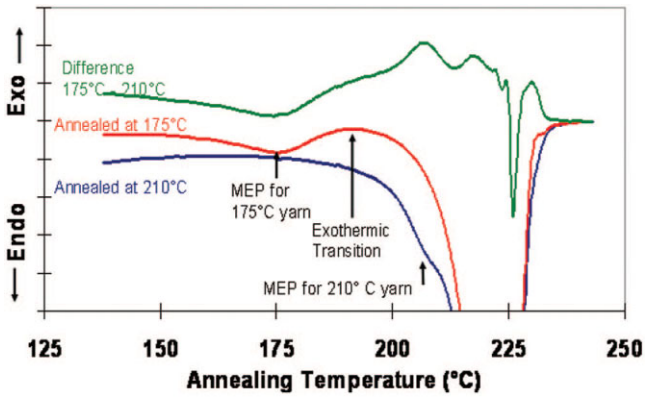

Figure 2 A different DSC trace obtained by subtracting DSC data of a fiber annealed at 210°C from that of a fiber annealed at 175°C. Also shown are the scans at 210 and 175°C. [Color figure can be viewed in the online issue, which is available at www.interscience.wiley.com.]

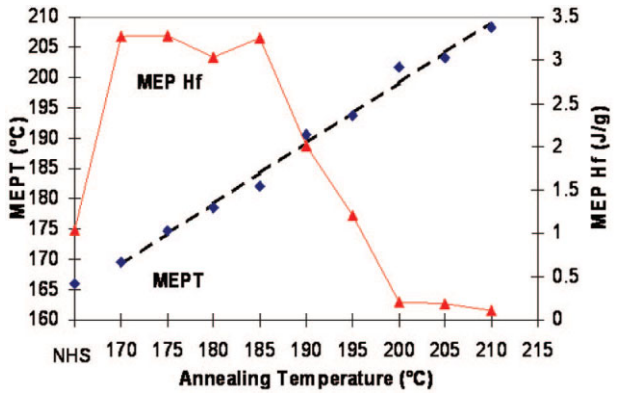

Figure 3 Changes in the peak temperature and the area of the MEP with annealing temperature. [Color figure can be viewed in the online issue, which is available at www.interscience.wiley.com.]

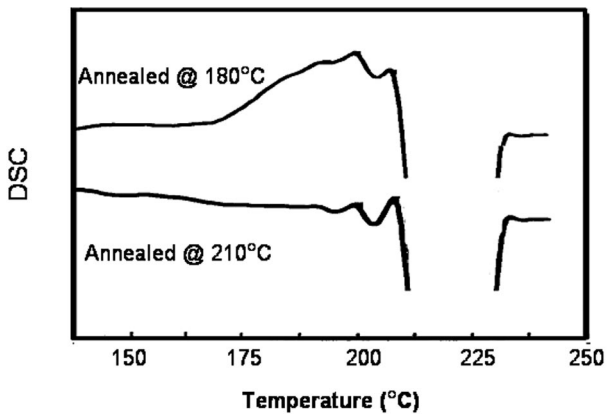

Figure 5 Oscillating DSC data showing the irreversible component in nylon 6 yarn annealed at two different temperatures.

X-ray analysis

Wide-angle XRD

The XRD scans showed that the crystalline phase in all the yarn samples were mostly α. A typical XRD scan with its resolved components is shown in Figure 6. The angular separation (in °2θ) between the two diffraction equatorial reflection at ~20° (α_1 peak, 200 reflection) and 24° (α_2 peak, 020 + 202 reflections), which we refer to as ICP, changes with annealing temperature as shown in Figure 7. The ICP initially decreases upon annealing at low temperatures and then slowly increases with annealing temperature from 170 to 180°C, showing an apparent discontinuity at about 185°C, and then continues to increase at significantly higher but constant rate at temperatures ≥195°C. Extrapolation of the linear regression fits to the data in two ranges, 170–180°C and ≥195°C, intersect at 190°C.

The CSP of the α_2 peak, as determined from its FWHM, is plotted as a function of annealing temperature in Figure 7 along with the ICP data. This plot shows that CSP initially decreases after annealing at a low temperature, remains essentially unchanged from 170 to 190°C, and then increases at an apparent constant rate at annealing temperatures >190°C.

Figure 8 shows the changes in the degree of crystalline orientation (f_c, from the 0140 reflection) with annealing temperature. f_c increases at a constant rate as the annealing temperature increases from 170 to 190°C and decreases at temperatures >190°C.

Small-angle X-ray scattering

Figure 9 shows that long-spacing and the integrated area of the lamellar peak increase with annealing temperature, after an initial decrease from the unannealed

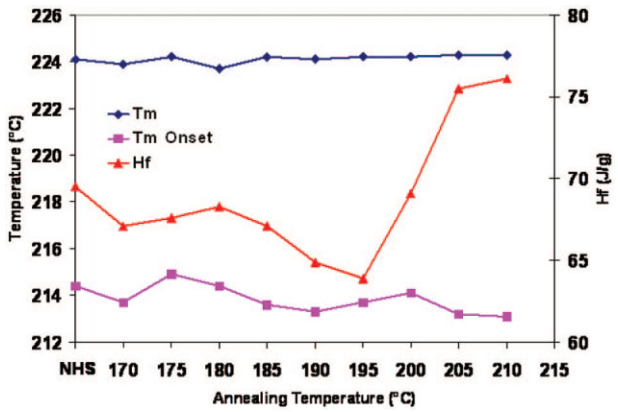

Figure 4 Parameters of the main melting peak in the DSC scan as a function of annealing temperature. Shown are the temperatures corresponding to melt point and onset of melting, and the heat of fusion. [Color figure can be viewed in the online issue, which is available at www.interscience.wiley.com.]

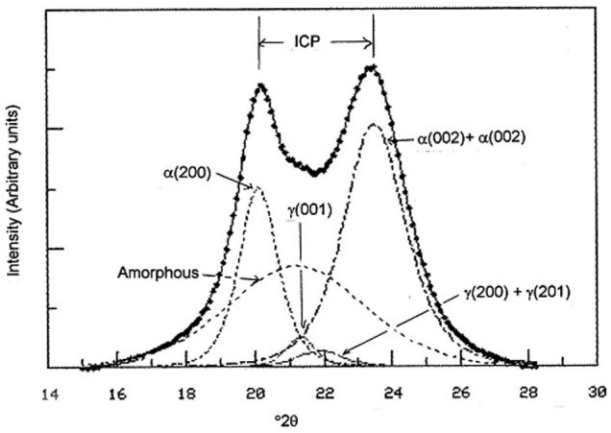

Figure 6 Typical profile analysis of the XRD scans to derive WAXD parameters.

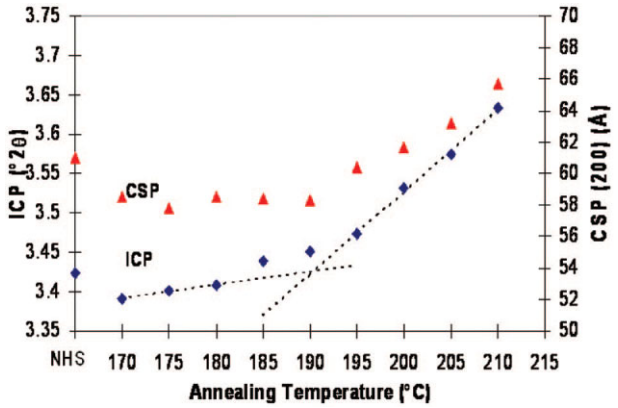

Figure 7 Changes in ICP and CSP (200 reflection) with annealing temperature. [Color figure can be viewed in the online issue, which is available at www.interscience.wiley.com.]

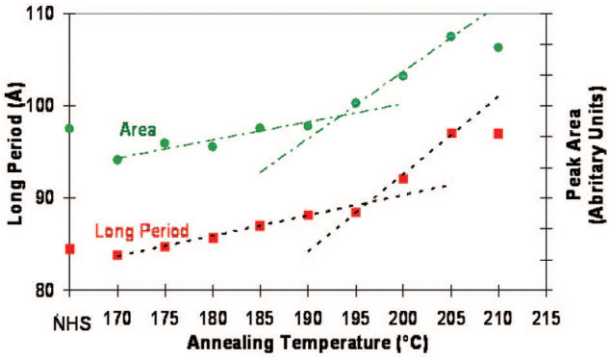

Figure 9 Changes in lamellar spacing (long period) and the lamellar intensity (peak area) with annealing temperature. [Color figure can be viewed in the online issue, which is available at www.interscience.wiley.com.]

yarn. Intercepts of the straight lines fitted to data below and above 190°C shows that these increases occur at a faster rate above 190–195°C. The values at 210°C appear to be same as or less than those at 205°C. The 210°C data points were not used in the high temperature fits. Figure 10 shows that the width of the peak along the fiber axis, corresponding to the coherence length of the lamellar stack, decreases with annealing temperature. Our SAXS data are similar to those reported by Hirami.[14]

Fiber properties

Figure 11 shows a typical dyeability data obtained using an acid blue dye from nylon 6 yarns heat-set at various Suessen (dry annealing) heat-set temperatures. Figure 12 shows the increase in the bulk density of the fibers upon annealing. The parabolic change in dyeability with heat setting temperatures in Suessen heat-set nylon 6,6 has been attributed to the competing effects of a decrease in free volume, which dominate at lower heat-set temperatures, and an increase in crystallinity, which dominate at higher temperatures.[15]

We also found that the change in percentage elongation as measured by TMA showed a parabolic shape similar to that of dyeability with a minimum at about 190°C and was consistent with prior results (unpublished Honeywell internal report, G. Turner, 1984).

DISCUSSION

Annealing or heat setting is widely used to alter the thermal history of a polymer, and thus controls polymer properties. The structural basis for these changes is still poorly understood. Semicrystalline polymers typically have domains of some limited order in addition to the commonly recognized amorphous and crystalline regions. These domains, which have been described as paracrystalline, poorly formed crystals, or small crystallites, melt at a lower temperature than the lamellar crystals, and thus give rise to the MEP. The detailed mechanisms of these permelting transitions have been discussed in detail[16] for polymers such as PET,[2,17] PPS, and PEEK.[5–7] While MEP is

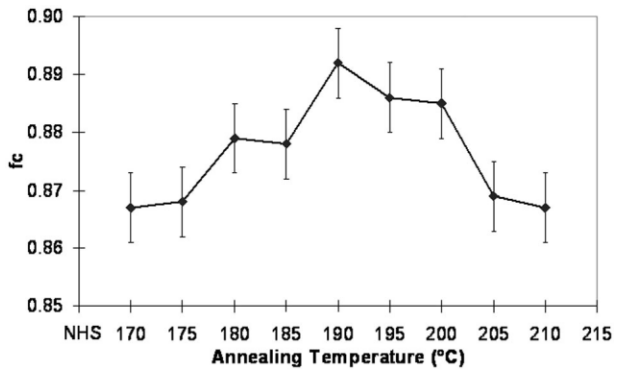

Figure 8 Changes in crystalline orientation with annealing temperature.

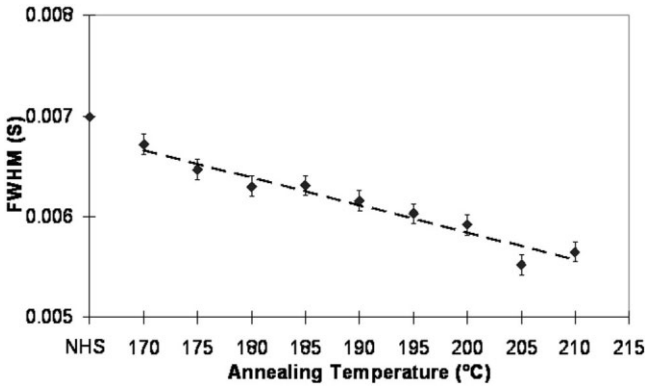

Figure 10 Decrease in the meridional width of the lamellar peak with increase in annealing temperature.

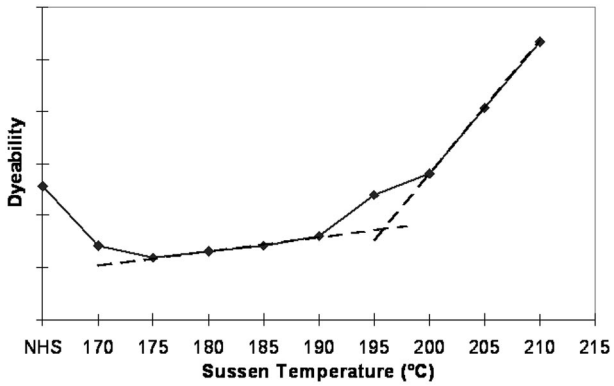

Figure 11 Typical dye level (acid dye) in dry-heat set (Suessen process) yarns.

always present, annealing brings about additional changes that can be attributed to secondary crystallization. A composite of all our data shows that the morphology of dry heat-set nylon 6 yarns changes dramatically when annealed at temperatures above 190°C (Fig. 13). This is indicated by a larger increase in ICP, CSP, long-spacing, and SAXS intensity in yarn and dyeability.[18] These increases are accompanied by exothermic peaks in DSC and thermal transitions in ODSC. We will discuss the significance of these transitions and correlate the MEP to material properties such as observed rapid changes in TMA elongation and the dyeability of Suessen heat-set (dry annealed) nylon 6 yarns.

These crystalline relaxations near 190°C has been speculated but never detected probably because of its close proximity to melting point in nylon 6.[9] This premelting exothermic peak has been reported for shock-cooled nylons, i.e., under combination of mechanical stresses rapid cooling, as is sometimes seen in melt extrudates in capillary rheometer. Addition of non-nucleating minerals such as laponite and montomorillonite enhances this transition.[8]

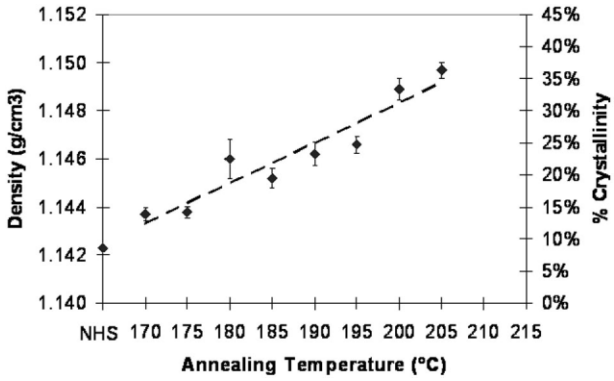

Figure 12 Increase in fiber density with annealing temperature.

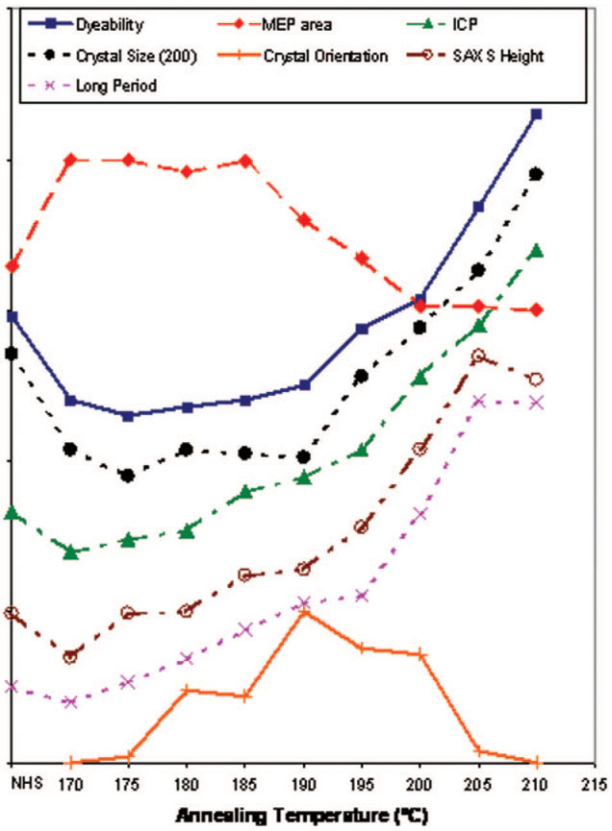

Figure 13 Composite of the various structural characteristics and the dyeability in various annealed yarns. [Color figure can be viewed in the online issue, which is available at www.interscience.wiley.com.]

Changes in morphology

The effects of annealing in fibers such as nylons have been interpreted in terms of two mechanisms, one related to formation and disappearance of small crystals and other to the thickening of existing crystals.[14] Our data, while in agreement with this simple model, provide details of the temperature ranges in which the two distinct mechanisms play a dominant role.

When nylon is annealed in a dry atmosphere at temperatures below 190°C, domains of limited order, most likely oriented amorphous domains, are able to relax and, because of limited chain mobility, they quickly reform into microcrystals. Using 3.5 J/g as the area under the MEP (Fig. 3) and 230 J/g for the heat of fusion of 100% crystalline nylon 6,[19] the weight fraction of these microcrystals can be calculated to be 1.5%. These new microcrystals remain embedded in the amorphous matrix outside the lamellar stack, restrict the mobility of amorphous chains, and decrease the permeability of guest molecules. This is the primary reason for the lighter dye uptake in dry heat-set yarns than in wet heat-set yarns. Microcrystals do not increase either the crystallinity as measured by wide-angle XRD or lamellar intensity as measured by SAXS.

Microcrystals being ~30 Å in size do not alter the nature of the wide-angle crystalline reflections, and their electron density is not much different from that of dense amorphous domains to affect the lamellar peak. As the annealing temperatures increases (up to 190°C), the average size or perfection of these microcrystals becomes larger, and correspondingly their MEPT increases.

The ICP, CSP, and lamellar-spacing and -intensity initially appear to decrease in NHS yarns upon annealing (Figs. 7 and 9). We have found that other parameters related to these and measured by several different techniques also decrease. This is puzzling because ICP and CSP rarely decrease upon annealing. This could be because ICP, CSP, long-spacing, and related parameters are the weighted average of the contributions from the crystalline lamellae and the newly created microcrystals. The decrease in these parameters for the NHS yarns is thus a direct evidence for the presence of microcrystals, especially in fibers annealed at 170, 175, and 180°C (Fig. 7). Note that in samples annealed below 190°C, ICP increases slightly while CSP remains essentially unchanged. This could be because ICP is more sensitive than CSP to morphological changes; ICP registers small changes within the crystal lattice accurately, while CSP tracks the over all changes in the size of and defect content within the crystal.

The onset of melting in the DSC scans is ~190°C (Fig. 1). This leads us to suggest that the microcrystals are unstable above 190°C, and the decrease in the MEP area in nylon 6 yarn annealed above 190°C is indicative of the decrease in the population of microcrystals. 190°C is probably the lowest temperature at which a crystal can melt. This mirrors the highest melting temperature, the equilibrium melting point (260°C for nylon 6), corresponding to perfect or infinite crystals.

Above 190°C, the CSP and the lamellar parameters begin to increase, as they should in a normal annealing process. The chain mobility within the crystalline stems at these temperatures is such that the chains from the surrounding amorphous matrix or microcrystals are incorporated into the crystalline lamellae. This is the crystal thickening process. The enhanced mobility may be due to the Brill transition that is reported to occur at ~180°C for nylon 6.[20–22] Increased chain mobility reduces the number of defects and the strain in the crystalline regions, and can account in part for the observed larger rate of increase in CSP, ICP, lamellar spacing, and intensity, and the decrease in crystalline orientation. Absence of MEP in fibers annealed at these temperatures (Fig. 3) shows that crystal thickening rather than the formation of microcrystals is the favored mechanism in fibers annealed above 190°C. As the amorphous domains are consumed, indicated by a small (5–10%) increase in the overall crystallinity as measured by density and XRD,[11] voids are expected to form amorphous regions. This and the roughness of the fibrillar surface account for the increase in the intensity of the equatorial streak seen in SAXS patterns of dry heat-set fibers.[23] A schematic of the proposed morphology in nonheat set fibers, and in fibers annealed at below 190°C and above 190°C, are shown in Figure 14.

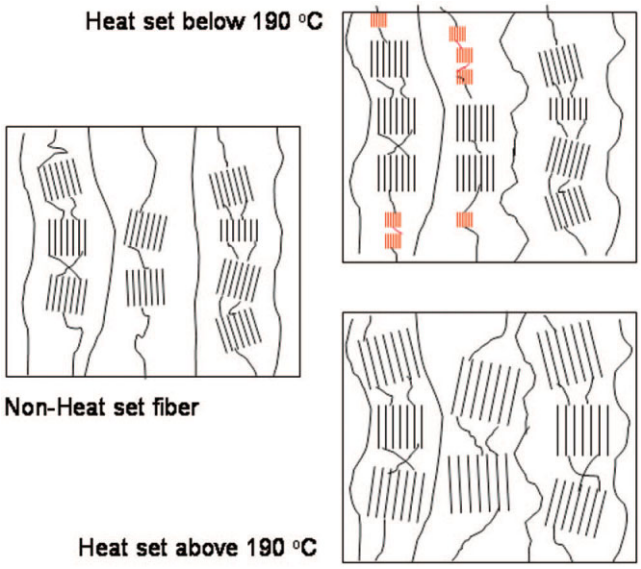

Figure 14 A schematic of the proposed morphological changes in fibers annealed below and above 190°C. [Color figure can be viewed in the online issue, which is available at www.interscience.wiley.com.]

The shift in the mechanism of development of crystallinity at 190°C coincides with the observed changes in the dyeability curve shown in Figure 11. Dyeability is a very sensitive, reliable, reproducible, and a powerful indicator of the small changes in the mobility of the dye molecules. Microcrystals and microvoids, both in the noncrystalline regions, affect dyeability in opposing ways; microcrystals hinder and microvoids aid in the diffusion of dyestuff. The increase in mobility of the polymer chains in the amorphous domains due to the lack of microcrystals in fibers annealed above 190°C would contribute to the formation of "more open amorphous regions" that are usually invoked to account for the increased dyeability. So also is the formation of microvoids as crystals thicken when annealed above 190°C by consuming amorphous chains. Our TMA data (unpublished), dyeability, and XRD data show that the trend seen at 190°C in the hot-air annealed yarns can be seen at temperatures as low as 120°C when annealing is done in wet-heat (Superba) or autoclave (wet steam). This is to be expected because thermal relaxation, including T_g, is shifted by 50–70°C in the presence of moisture.[24,25]

Crystalline orientation and microcrystals

The changes in the crystalline orientation upon annealing depend on the annealing temperature as well

as the orientation in the precursor fibers. We have previously noticed that in highly oriented fibers ($f_c >$ 0.95), the crystalline orientation decreases upon annealing at all temperatures,[18] but in the less oriented fibers used in this study ($f_c < 0.94$), the crystalline orientation increases at temperature <190°C, and decreases at higher temperatures. Decrease in crystalline orientation upon annealing above 190°C can be attributed to large scale reorganization of the lamellae resulting from increased mobility in the amorphous domains discussed earlier. The driving force is the thermodynamic tendency to achieve the less oriented, higher entropic state. At low annealing temperatures, in poorly oriented fibers, we speculate that microcrystals formed at the expense of amorphous chains within a fibril and between the lamellar stacks (Fig. 14). These microcrystals can be expected to provide sufficient force to orient the lamellar stacks within the fibril, and thus increase the crystalline orientation. The microcrystal-induced orientation is also the likely cause of the increase in length observed during aging-induced crystallization of as-spun, poorly oriented fibers with very low crystallinity (as-spun fibers ~15% crystallinity).

The heat of fusion (H_f') associated with MEP depends on the degree of orientation in the precursor fibers. For example, at an annealing temperature of 175°C, H_f' in highly oriented fibers is about one-fourth of that in less oriented fibers (f_c : 0.97 versus 0.93; H_f': 0.884 versus 3.29 J/g). However, H_f' is about the same in the two fibers when annealed at 200°C (0.145 versus 0.200 J/g). The low value of heat of fusion at lower temperature is consistent with the model proposed earlier for the formation of microcrystals from amorphous chains between the lamellar stacks within a fibril. The particular fiber we studied (4.5X drawn fiber) has 26% unoriented amorphous fraction when compared with 49% in the less oriented fibers.[11] Both have similar oriented amorphous fractions (27% in highly drawn and 24% in dawn fibers with lower draw ratios). On the basis of the commonly used model that oriented fractions lie between the fibrils, these values support the idea that microcrystals are formed between lamellar stacks within a fibril at the expense of the unoriented amorphous chains (Fig. 14). Although these microcrystals increase the orientation in less oriented fibers when annealed below 190°C, the resulting forces from fewer microcrystals in highly drawn fibers are apparently insufficient to resist the effect of the disorienting amorphous chains between the fibrils to decrease the overall crystalline orientation.

CONCLUSIONS

Microcrystals are formed at the expense of the unoriented amorphous chains between the lamellae within a fibril in fibers annealed below 190°C. These microcrystals give rise to the premelting endotherms and inhibit the mobility of polymer chains in both the amorphous and crystalline domain, and the mobility of dyes stuff while increasing the crystalline orientation in fibers with $f_c < 0.95$. Lamellar growth occurs in fibers annealed above 190°C as observed by the absence of a premelting exothermic transition and by rapid increase in crystalline density, crystallite size, long-spacing, and SAXS peak intensity. These increases along with rapid increases in ICP above 190°C are attributed to the onset of relaxations within the lamellae.

The authors thank J. Belles and H. Ashworth Jr. for collecting the DSC data, C. W. Walston for the XRD data, A. J. Redfern for supplying the yarn, and B. Waring for annealing the yarns.

References

1. Mandelkern, L. Crystallization of Polymers, Vols. I and II; Cambridge University Press: Cambridge, 2002 and 2005.
2. Oswald, H. J.; Turi, E. A.; Harget, P. J.; Khanna, Y. P. J Macromol Sci Phys 1977, B13, 231.
3. Khanna, Y. P. J Appl Polym Sci 1990, 40, 569.
4. Reading, M.; Elliott, D.; Hill, V. Proceedings of the 21st NATAS 1992, 145.
5. Lattimer, M. P.; Hobbs, J. K.; Hill, M. J.; Barham, P. J. Polymer 1992, 33, 3971.
6. Blundell, D. J. Polymer 1987, 28, 2248.
7. Lee, Y.; Porter, R. S. Macromolecules 1987, 20, 1336.
8. Khanna, Y. P. Macromolecules 1992, 25, 3298.
9. Murayama, T. Dynamic Mechanical Analysis of Polymeric Materials; Elsevier: New York, 1978.
10. Murthy, N. S.; Minor, H. Polymer 1990, 31, 996.
11. Murthy, N. S.; Bray, R. G.; Correale, S. T.; Moore, R. A. F. Polymer 1995, 36, 3863.
12. Heuvel, H. M.; Huisman, R. J Polym Sci Polym Phys Ed 1981, 19, 121.
13. Murthy, N. S.; Minor, H. Polym Commun 1991, 32, 297.
14. Hirami, M. Makromol Chem 1967, 105, 296.
15. Baxley, Jr., R. V.; Miller, R. W. Text Res J 1991, 61, 697.
16. Nichols, M. E.; Robertson, R. E. J Polym Sci Part B: Polym Phys 1992, 30, 305.
17. Zhou, C.; Clough, S. B. Polym Eng Sci 1988, 28, 65.
18. Murthy, N. S.; Minor, H.; Latif, R. A. J Macromol Sci Phys 1987, B26, 427.
19. Khanna, Y. P.; Kuhn, W. P. J Polym Sci Part B: Polym Phys 1997, 35, 2219.
20. Murthy, N. S.; Curran, S. A.; Aharoni, S. M.; Minor, H. Macromolecules 1991, 24, 3215.
21. Vasanthan, N.; Murthy, N. S.; Bray, R. G. Macromolecules 1998, 31, 8433.
22. Ramesh, C.; Bhoje Gowd, E.. Macromolecules 2001, 34, 3308.
23. Murthy, N. S.; Reimschuessel, A. C.; Kramer, V. J Appl Polym Sci 1990, 40, 249.
24. Murthy, N. S. Int J Polym Mat 2001, 50, 429.
25. Murthy. N. S.; Akkapeddi, M. K.; Orts, W. J. Macromolecules 1998, 31, 142.